Selection and suppression of soft x-ray spectral features using optimized multilayer coatings

2001 J. Opt. A: Pure Appl. Opt. 3 61

(http://iopscience.iop.org/1464-4258/3/1/310)

INSTITUTE OF PHYSICS PUBLISHING JOURNAL OF OPTICS A: PURE AND APPLIED OPTICS
J. Opt. A: Pure Appl. Opt. **3** (2001) 61–66 www.iop.org/Journals/oa PII: S1464-4258(01)14344-8

Selection and suppression of soft x-ray spectral features using optimized multilayer coatings

A G Michette[1] **and Z Wang**[1,2]

[1] Department of Physics, King's College London, Strand, London WC2R 2LS, UK
[2] State Key Laboratory of Applied Optics, Changchun Institute of Optics, Fine Mechanics and Physics, Chinese Academy of Sciences, PO Box 1024, Changchun 130022, People's Republic of China

Received 26 May 2000, in final form 10 October 2000

Abstract
The design of multilayer mirrors which specifically select or suppress spectral features is described. To illustrate the method, the spectra from laser-produced plasmas of carbon and aluminium are used. By using a suitable mirror the intensity of the C V He_α line at $\lambda = 4.03$ nm can be reduced to 1.1×10^{-4} of that in the C VI Ly_α line at $\lambda = 3.37$ nm, compared to 0.97 in the source emission spectrum and 1.6×10^{-2} for a periodic multilayer. In the aluminium spectrum, two closely spaced lines at $\lambda = 3.505$ and 3.660 nm, which have comparable emitted intensities, can be individually selected using pairs of multilayers. The reflected intensity ratios are under ten for periodic multilayers, but can be over 300 for the shorter wavelength line and almost 140 for the longer using optimized pairs of mirrors.

Keywords: Depth-graded multilayer mirrors, soft x-ray and EUV optics, wavelength-selective x-ray optics

1. Introduction

In previous papers the designs of depth-graded x-ray multilayer mirrors with broad angular [1] or wavelength [2] responses have been described. In addition, the problems of enhancing the throughput (the product of source intensity and reflectivity) or selectivity (maximized throughput in a given range coupled with minimum throughput outside that range) have been addressed [3] for sources emitting essentially continuum radiation over a given wavelength range. The method used was a stochastic one in which, starting from a particular layer distribution (which could either be a periodic multilayer or the results of a previous calculation), the position of a random boundary was shifted by a random amount. If this resulted in the improvement of some merit function the change was kept; otherwise it was rejected. This process was continued until the merit function was optimized.

In the current paper, the concept of enhancing the throughput is widened to the problem of picking out specific spectral lines from a source emitting a line spectrum. Additionally, the idea of selectivity is broadened to encompass maximizing the throughput for a specific spectral line while minimizing that for nearby spectral lines. Here, the interest is in line sources emitting in the wavelength region between the oxygen and carbon K_α absorption edges at 2.3 and 4.47 nm respectively, the 'water window', which is a suitable range for the x-ray imaging of hydrated specimens. In principle these calculations can be performed for normal-incidence mirrors but, because the optimum number of bilayers is then about 200, the computation time is very long. A glancing angle of 20° was therefore used instead, for which about 60 layer pairs is optimum. The spectrum (figure 1) of a laser-plasma source with a carbon target is used in section 2 for the design of a tungsten/scandium multilayer with high throughput in a small range (±0.05 nm) about the C VI Ly_α line at $\lambda = 3.37$ nm, which contains 45% of the total flux. The spectrum was extracted from that measured with a Mylar target [4], using a transmission grating with low spectral resolution but well characterized efficiency to give the relative intensities of the spectral lines and a flat-field spectrometer to give a better measurement of the line widths, which are predominantly instrumental. The performance of the optimized mirror is also compared with that of a periodic multilayer.

In section 3 the same source spectrum is used in the design of W/Sc multilayers with high selectivity for the C VI Ly_α line.

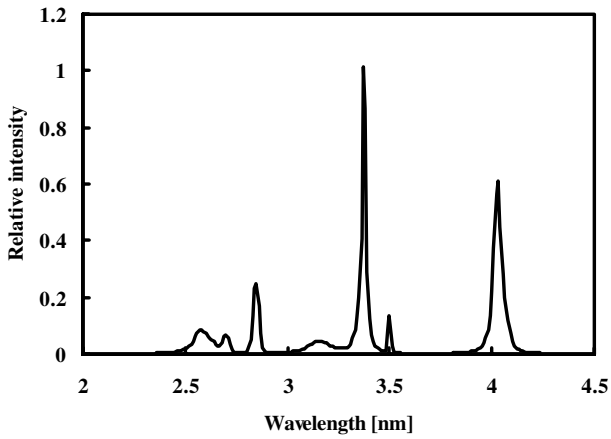

Figure 1. The emission spectrum of a laser-plasma source with a carbon target.

Table 1. The relative intensities of the strongest features in the carbon laser-plasma spectrum.

Feature	Wavelength range (nm)	Relative intensity
Recombination edge	2.53–2.63	0.22
C VI Ly_γ line	2.65–2.75	0.12
C VI Ly_β line	2.80–2.90	0.29
C VI Ly_α line	3.32–3.42	1
C V He_β line	3.45–3.55	0.10
C V He_α line	3.98–4.08	0.97

The selectivity is defined in several ways, first for the integrated spectral intensity outside 3.37 ± 0.05 nm and then for ranges of ± 0.05 nm around one or more other lines in the spectrum. The strongest spectral features are at ∼2.58 nm (a recombination edge), 2.7 nm (C VI Ly_γ line), 2.85 nm (C VI Ly_β line), 3.5 nm (C V He_β line) and 4.03 nm (C V He_α line). The intensities of these features, relative to that of the C VI Ly_α line, are shown in table 1.

Although, as will be seen, multilayers with the required performance characteristics can be designed, they will not necessarily be useful in practice. This is because the range of applications of x-ray microscopic imaging at a specific wavelength is limited. It is often more useful to be able to take images at two or more closely separated wavelengths, so that comparison of the images can lead to elemental or chemical state mapping [5]. In section 4 pairs of multilayers are described which were designed to select one of two closely spaced lines in an aluminium laser-plasma spectrum, while suppressing the second line and other spectral features.

For all the calculations interfacial roughnesses of 0.3 nm and zero boundary position errors are assumed, and the boundaries are assumed to be sharp since experimentally achievable tolerances do not have major effects [2].

2. High-throughput, narrow-bandpass multilayer

For maximum throughput in a given wavelength range with a source spectrum $S(\lambda)$ the merit function that should be maximized is

$$MF_{\text{throughput}} = \int_{\lambda_{\min}}^{\lambda_{\max}} T(\lambda)\,\mathrm{d}\lambda \qquad (1)$$

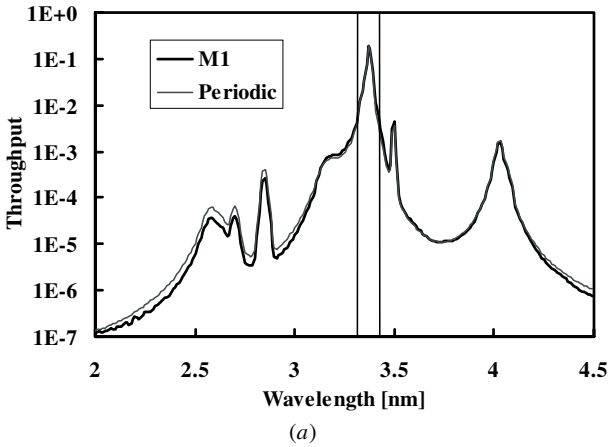

(*a*)

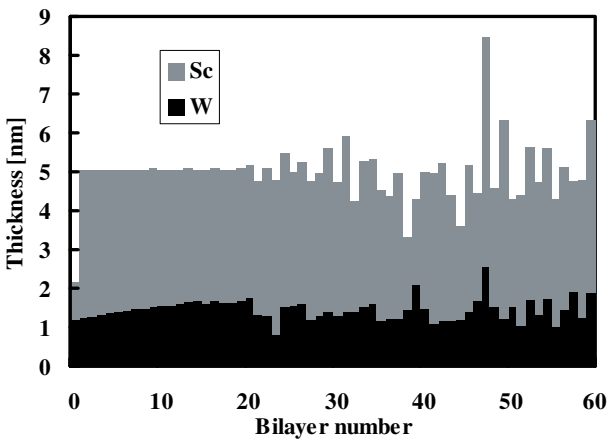

(*b*)

Figure 2. (*a*) The throughput of a W/Sc multilayer (M1) optimized for maximum throughput in the C VI Ly_α line at 3.37 nm, indicated by the vertical lines. The throughput of a periodic multilayer is also shown. (*b*) The corresponding distribution of layer thicknesses, with bilayer number increasing downwards from the top of the multilayer stack. The full bilayer thicknesses are given by the overall heights of the bars, and the individual tungsten or scandium thicknesses by the heights of the appropriately shaded parts.

where the throughput is $T(\lambda) = R(\lambda)S(\lambda)$ and $R(\lambda)$ is the reflectivity as a function of wavelength. Using the spectrum shown in figure 1, a multilayer (mirror M1) was designed for the wavelength range 3.32–3.42 nm to select the C VI Ly_α line at $\lambda = 3.37$ nm. Figure 2(*a*) shows the throughputs of M1 and of a periodic multilayer designed for maximum reflectivity at $\lambda = 3.37$ nm. The integrated reflectivity of mirror M1 in the defined wavelength range is 1.10 ± 0.30 times that of the periodic multilayer and the throughput is 3% higher. The slight increase in the throughput results from enhancement away from the spectral line peak; the throughput is also increased for some spectral features close to but outside the required wavelength range, which may be undesirable. The selectivity of mirror M1, i.e. the ratio of the throughputs inside and outside the range, is 11.4, slightly worse than the value of 11.9 for the periodic mirror; the corresponding improvements over the bare source spectrum are by factors of 25 and 26.5, respectively. The slight worsening of the selectivity for mirror M1 is not a cause for concern, since the merit function used here did not include selectivity; the values are given here for comparison with later results.

The periodic multilayer has a tungsten (more absorbing) thickness of 1.25 nm and a scandium (less absorbing) thickness of 3.75 nm in each bilayer, i.e. a period of 5 nm. The layer thickness distribution of mirror M1 is shown in figure 2(*b*); the average tungsten and scandium thicknesses are 1.26 ± 0.28 and 3.51 ± 0.67 nm, respectively, and the average bilayer thickness is 4.96 ± 0.77 nm. Apart from a thin top bilayer (2.17 nm), mainly due to the small scandium thickness (0.99 nm), the first 20 bilayers have a roughly constant thickness (5.05 ± 0.02 nm) with a gradually increasing tungsten thickness and a gradually decreasing scandium thickness. The thicknesses then start to oscillate, with the major oscillations being in the scandium layers. It is these oscillations which cause the differences in performance between M1 and the periodic multilayer.

3. High-throughput, selective-bandpass multilayers

For a multilayer with high throughput in a given wavelength range and minimum throughput outside that range the merit function to be maximized is

$$MF_{\text{selectivity}} = \frac{\int_{\lambda_{\min}}^{\lambda_{\max}} T(\lambda)\,\mathrm{d}\lambda}{\sum_i \int_{\lambda_{1i}}^{\lambda_{2i}} T(\lambda)\,\mathrm{d}\lambda} \qquad (2)$$

where $\lambda_{\min}$ and $\lambda_{\max}$ define the required wavelength range, the sum is over all regions of the spectrum for which minimum throughput is required and λ_{1i} and λ_{2i} define the lower and upper bounds to the ith region.

3.1. Minimum integrated throughput outside the defined range

Using the merit function of equation (2) a multilayer (mirror M2) was designed to given maximum throughput in the range 3.32–3.42 nm with minimum integrated throughput outside that range. Figure 3 shows the throughput of this multilayer, and that of the periodic multilayer. The integrated reflectivity and throughput of mirror M2 in the defined wavelength range are close to those of the periodic multilayer, but the selectivity has increased to 20.2, a factor of 45 better than the bare source spectrum and 70% higher than the periodic multilayer. In addition to this improved selectivity, figure 3 shows that the optimization procedure has led to reduced throughputs in the neighbourhood of other strong spectral features, particularly the line at 4.03 nm. This suggests that minimizing the throughput around particular features can lead to better suppression of those features.

The different performances of mirrors M1 and M2 are clearly related to the lower layers in which the thickness oscillations take place, even though only about 6 and 9% of the incident radiation in the range 3.32–3.42 nm penetrates the top 20 bilayers of M1 and M2, respectively. If the oscillations are smoothed out, and the layer thicknesses are replaced with the average values, the mirror performances approach those of the periodic multilayer. Additionally, if just the major oscillations are removed then the throughputs in the required wavelength range and (for M2) selectivity are also degraded.

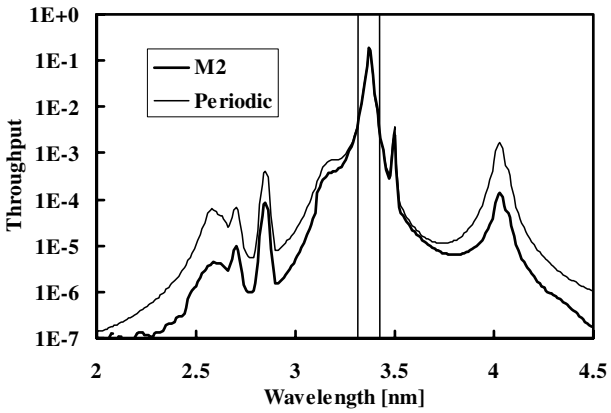

Figure 3. The throughput of a W/Sc multilayer (M2) optimized for maximum throughput in the C VI Ly_α line at 3.37 nm, indicated by the vertical lines, with minimum integrated throughput elsewhere. The throughput of a periodic multilayer is also shown.

3.2. Suppression of spectral features

The carbon laser plasma spectrum has several lines, other than the strongest at a wavelength of 3.37 nm, which could cause, for example, blurring or spectral contamination of images in x-ray microscopy. It is therefore of interest to see whether multilayers can be designed to specifically suppress spectral features while maintaining high throughput at the desired wavelength. Mirrors M3–M8 were designed, using equation (2), to give high throughput for the range $\lambda_{\min}$–$\lambda_{\max}$ = 3.32–3.42 nm with minimum throughput in the range ± 0.05 nm around the peaks of one or more other spectral features (table 2). The results are summarized in table 3.

The results show that it is possible to suppress efficiently specific spectral features. For example, mirror M3, which was designed to suppress the C V He_α line at 4.03 nm, has a throughput in this line of 1.1×10^{-4}, relative to that for the C VI Ly_α line where the throughput was maximized. This is to be compared with 0.97 for the source spectrum, 1.6×10^{-2} for the periodic multilayer and 1.4×10^{-2} for the maximized throughput mirror M1. Mirror M4, designed to suppress the C V He_β line at 3.5 nm, does not perform so well due to the proximity of the maximized and minimized features, but even so has a relative throughput of 7.2×10^{-3}, compared to 0.1, 1.6×10^{-2} and 1.8×10^{-2} for the source, periodic multilayer and M1, respectively.

Mirrors designed to suppress two features (M5 and M6) can also work well, as shown in table 3, particularly if both features are well removed from the feature to be maximized, as is the case for mirror M6. However, if more than two features are suppressed the performance can begin to degrade, as shown in table 3 for mirrors M7 and M8 compared to M2. This suggests that, unless the aim is to suppress specific strong lines, it may be better to minimize the integrated throughput.

4. Multilayer pairs for selection and suppression of two closely spaced spectral lines

In order to carry out elemental mapping using an x-ray microscope on a laser-plasma source, it is necessary to form the plasma from a material giving a spectrum with several

Table 2. Design criteria of the multilayer mirrors for the carbon laser-plasma spectrum. All were designed for maximum throughput in the range ±0.05 nm around the C VI Ly_α line at $\lambda = 3.37$ nm.

Mirror	Throughput minimized
M1	None
M2	Integrated outside 3.32–3.37 nm
M3	C V He_α
M4	C V He_β
M5	C V He_α and C V He_β
M6	C VI Ly_β and C V He_α
M7	C V He_α, C V He_β and C VI Ly_β
M8	C V He_α, C V He_β, C VI Ly_β, C VI Ly_γ and recombination edge

Table 3. Relative throughputs of the mirrors for the different spectral features of the carbon laser-plasma spectrum. For the C VI Ly_α line the throughput is given relative to the source output while for all other features it is given relative to that of the C VI Ly_α line for that mirror; this is equivalent to the inverse of the selectivity.

	Periodic	M1	M2	M3	M4	M5	M6	M7	M8
C VI Ly_α line	0.58	0.59	0.58	0.57	0.56	0.57	0.59	0.58	0.57
Recombination edge	8.9×10^{-4}	5.1×10^{-4}	7.0×10^{-5}	2.7×10^{-4}	5.3×10^{-4}	1.5×10^{-4}	9.8×10^{-5}	2.2×10^{-4}	1.6×10^{-4}
C VI Ly_γ line	6.5×10^{-4}	3.8×10^{-4}	8.7×10^{-5}	3.0×10^{-4}	6.2×10^{-4}	1.1×10^{-4}	8.7×10^{-5}	2.7×10^{-4}	1.3×10^{-4}
C VI Ly_β line	2.8×10^{-3}	1.7×10^{-3}	5.6×10^{-4}	2.2×10^{-3}	2.2×10^{-3}	8.5×10^{-4}	7.8×10^{-6}	5.7×10^{-4}	5.8×10^{-4}
C V He_β line	1.6×10^{-2}	1.8×10^{-2}	1.2×10^{-2}	1.8×10^{-2}	7.2×10^{-3}	9.3×10^{-3}	1.5×10^{-2}	9.4×10^{-3}	8.1×10^{-3}
C V He_α line	1.6×10^{-2}	1.4×10^{-2}	1.4×10^{-3}	1.1×10^{-4}	2.2×10^{-2}	1.0×10^{-3}	1.1×10^{-4}	2.0×10^{-3}	8.5×10^{-4}
Integrated	0.084	0.088	0.049	0.070	0.099	0.064	0.059	0.069	0.063

Table 4. Comparison of the multilayer mirrors designed for the aluminium laser-plasma spectrum.

Wavelength of line (nm)	Relative intensity in spectrum	Throughput relative to selected feature (A, 3.505 nm or B, 3.660 nm)					
		Periodic (A)	Periodic (B)	M9 (A)	M10 (B)	M11 (A)	M12 (B)
3.300	0.89	0.096	0.038	0.469	0.243	0.058	9.37×10^{-3}
3.505	1	1	0.217	1	7.34×10^{-3}	1	0.143
3.660	0.90	0.126	1	3.23×10^{-3}	1	0.066	1
3.915	1.23	0.031	0.080	0.180	0.354	8.84×10^{-3}	0.055

closely spaced lines. For this elements of medium Z are suitable, for example aluminium, for which the spectrum is as shown in figure 4. This spectrum is of interest since it has two strong lines, at 3.505 nm due to Al XI and 3.660 nm due to Al X, on either side of the calcium L absorption edge; the transmission of 1 μm of calcium is also shown in figure 4, ignoring fine structure near the absorption edge. A multilayer which reflects the 3.505 nm line and suppresses the 3.660 nm line will therefore allow an image to be made at a wavelength for which calcium is absorbing, whereas one which reflects the 3.660 nm line and suppresses the 3.505 nm line will enable an image to be formed at a wavelength for which calcium is transmitting. Comparison of the two images then allows a map of the calcium distribution in the sample to be made [5], since the transmission of other elements does not vary rapidly near to the calcium edge [6].

Mirrors M9 and M10 were designed to enhance the lines at 3.505 and 3.660 nm, respectively. Unlike the mirrors designed for the carbon spectrum the layer thickness distributions show oscillations throughout the full multilayer stack. The throughputs of the two mirrors are compared in figure 5(*a*), and those of the corresponding periodic multilayers in figure 5(*b*). These demonstrate the improved performances of M9 and M10 in suppressing the unwanted line. In the spectrum the ratio of the intensities in the 3.505 and 3.660 nm lines is 1.11, while mirror M9 gives a throughput ratio of 309, an improvement

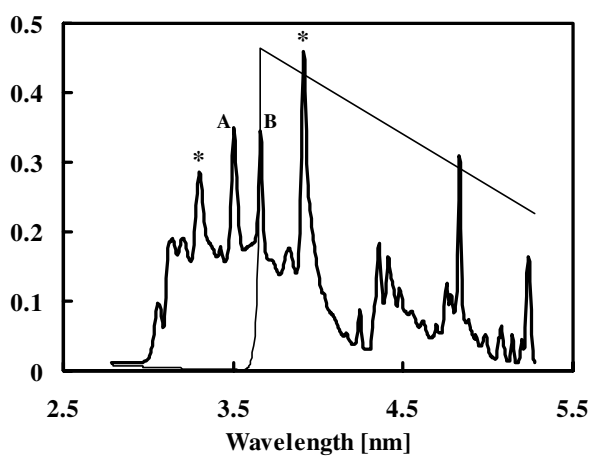

Figure 4. The emission spectrum of a laser-plasma source with an aluminium target (thick curve). Also shown is the transmission of 1 μm of calcium, showing that the line at $\lambda = 3.505$ nm (A) lies just on the absorbing side of the calcium L edge while that at 3.660 nm (B) lies on the transmitting side. The two lines indicated by asterisks were also included in the optimization of one mirror pair (M11 and M12).

by a factor of 278 over the spectrum and by a factor of 35 over the corresponding periodic multilayer. Mirror M10 gives a ratio of throughputs in the 3.660 and 3.505 nm lines of 136,

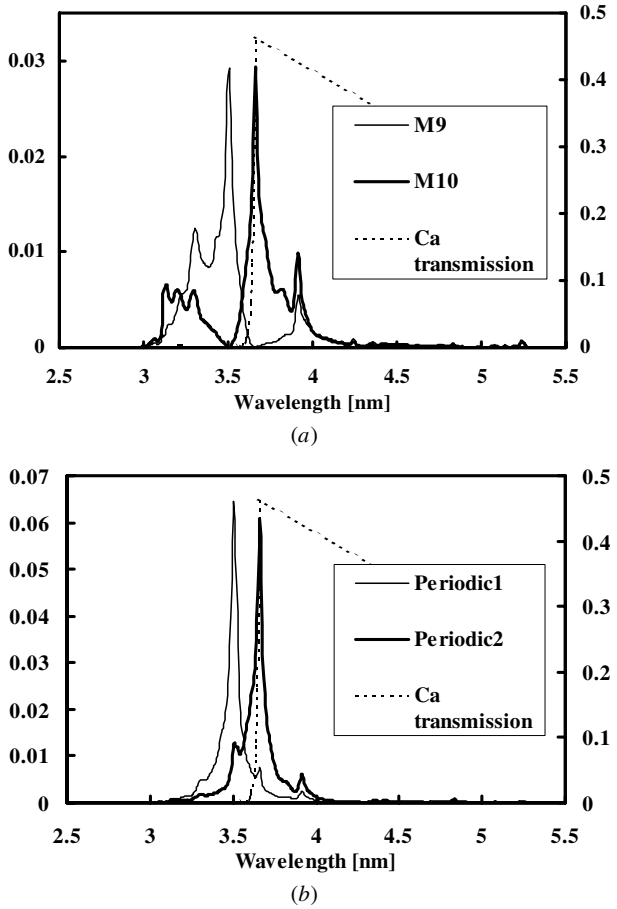

Figure 5. (*a*) The throughputs of mirrors M9 and M10 (left-hand axis) and the transmission of 1 μm of calcium (right-hand axis). (*b*) The corresponding curves for the periodic multilayers.

an improvement by a factor of 152 over the spectrum and by a factor of 33 over the corresponding periodic multilayer, which gives a throughput ratio of just over 4.

However, comparison of figures 5(*a*) and (*b*) shows that the periodic mirrors suppress other spectral features better than mirrors M9 and M10 do. Two further mirrors (M11 and M12) were therefore designed to suppress other nearby strong lines in the spectrum, specifically those at 3.300 nm (Al XI) and 3.915 nm (two unresolved Al XI lines), marked with an asterisk in figure 4; their performances, shown in figure 6, are better than both M9 and M10 and the periodic mirrors. The performances of all the mirrors for the aluminium spectrum are compared in table 4.

5. Conclusions and discussion

It has been demonstrated that, by using a stochastic design process to determine the optimum layer thickness distributions, multilayer mirrors which are much more versatile than periodic ones can be designed. Previously [1] it has been shown that the method also gives better results than those based on power-law variations of the layer thicknesses [7]. The mirrors have potential applications in many fields where it may be desirable to enhance or suppress certain spectral features, including elemental mapping in x-ray microscopy. Care must be taken

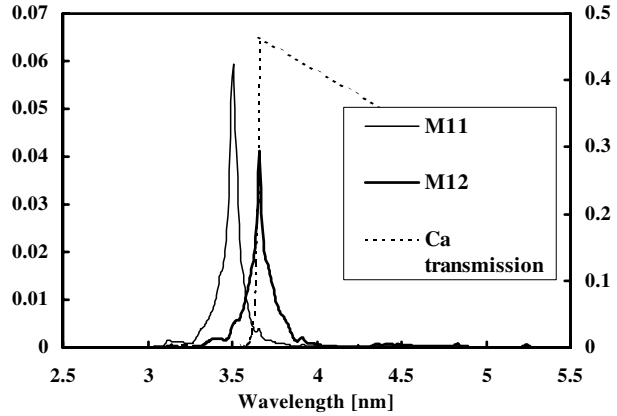

Figure 6. The throughputs of mirrors M11 and M12 (left-hand axis) and the transmission of 1 μm of calcium (right-hand axis).

during the design to use a suitable merit function to give the required performance of the multilayer.

One drawback of the method is that there are no apparent correlations between the required performances and the calculated layer thickness distributions. It is clearly the layer thickness oscillations which result in the required performances, since removing just one of the major oscillations significantly degrades the performance. If such a correlation could be found, even if it were a weak one, it could provide suitable starting points in the design process, which at present can be computationally expensive.

However, comparison of the layer thickness distributions of, for example, mirrors M9 and M10 or M11 and M12 does not provide any obvious clues to their performance differences. For multilayers designed to reflect at single wavelengths but with defined angular responses [1], it is easier to find correlations since then only a single set of optical constant values (refractive index n and absorption index β) is required. Indeed, some methods of designing such multilayers use bilayer thickness distributions approximated from the inverse Fourier transform of the required angular response [8]. However, for multilayers with defined wavelength responses, this approach is not readily tractable, since both n and β vary with wavelength so that values are required over the whole wavelength range of interest. Although functional forms of n and β can be derived [9] these are often not in very good agreement with experiment [6]; the best approach may be to use functions fitted to the experimental values but even then it can be envisaged that the approach could only give approximate results. In addition, if it is the throughput response which is to be optimized as is the case here, rather than just the reflectivity, it would be necessary to include a function defining the source spectrum in the analysis. For a continuum spectrum, as described previously [3], this may be possible, but a complicated line spectrum would require too many parameters.

Acknowledgment

This study is financially supported in part by the National Natural Science Foundation of China for General Scientific Research, contract no 69778026 to Zhanshan Wang.

References

[1] Wang Z, Cao J and Michette A G 2000 Depth-graded multilayer x-ray optics with broad angular response *Opt. Commun.* **177** 25–32

[2] Michette A G and Wang Z 2000 Optimisation of depth-graded multilayer coatings for broadband reflectivity in the soft x-ray and EUV regions *Opt. Commun.* **177** 47–55

[3] Wang Z and Michette A G 2000 Broadband multilayer mirrors for optimum use of soft x-ray source output *J. Opt. A: Pure Appl. Opt.* **2** 452–7

[4] Michette A G and Pfauntsch S J 2000 *J. Phys. D: Appl. Phys.* **33** 1186–90

[5] Buckley C J, Khaleque N, Bellamy S J, Robins M and Zhang X 1998 Mapping the organic and inorganic components of bone *X-Ray Microscopy and Spectromicroscopy* (Berlin: Springer) pp II-47–55

[6] Henke B L, Gullikson E M and Davis J C 1993 X-ray interactions: photoabsorption, scattering, transmission, and reflection at $E = 50$–$30\,000$ eV, $Z = 1$–92 *At. Data Nucl. Data Tables* **54** 181–342

[7] Joensen K D, Voutov P, Szentgyorgyi A, Roll J, Gorenstein P, Høghøj P and Christensen F E 1995 Design of grazing-incidence multilayer supermirrors for hard x-ray reflectors *Appl. Opt.* **34** 7935–44

[8] Protopopov V V and Kalnov V A 1998 X-ray multilayer mirrors with an extended angular range *Opt. Commun.* **158** 127–40

[9] Michette A G 1986 *Optical Systems for Soft X-Rays* (New York: Plenum)